Coherent Vector-Meson Photoproduction with Nuclear Breakup in Relativistic Heavy-Ion Collisions

Anthony J. Baltz,[1] Spencer R. Klein,[2] and Joakim Nystrand[3]

[1]*Brookhaven National Laboratory, Upton, New York 11973*
[2]*Lawrence Berkeley National Laboratory, Berkeley, California 94720*
[3]*Department of Physics, Lund University, Lund SE-22100, Sweden*

(Received 10 May 2002; published 14 June 2002)

Relativistic heavy ions are copious sources of virtual photons. The large photon flux gives rise to a substantial photonuclear interaction probability at impact parameters where no hadronic interactions can occur. Multiple photonuclear interactions in a single collision are possible. In this Letter, we use mutual Coulomb excitation of both nuclei as a tag for moderate-impact-parameter collisions. We calculate the cross section for coherent vector-meson production accompanied by mutual excitation and show that the median impact parameter is much smaller than for untagged production. The vector-meson rapidity and transverse-momentum distribution are very different from untagged exclusive vector-meson production.

DOI: 10.1103/PhysRevLett.89.012301 PACS numbers: 25.75.Dw, 12.40.Vv, 25.20.Lj

The large charge (Z) of heavy nuclei gives rise to strong electromagnetic fields. For relativistic nuclei, these fields may be treated as an almost-real virtual photon beam, following the Weizsäcker-Williams method. In relativistic heavy ion collisions, the photon field of one nucleus can produce a photonuclear interaction in the other. Many types of photonuclear interactions are possible: nuclear excitation, coherent or incoherent vector-meson production, and other incoherent photonuclear interactions [1]. When the impact parameter b is significantly larger than twice the nuclear radius R_A, hadronic interactions are not possible, and photonuclear reactions can be cleanly detected. When $b > 2R_A$, the absolute probability for many of the photonuclear reactions can be substantial, and, consequently, multiple reactions are possible. For example, each ion can emit a photon, exciting the other nucleus, leading to mutual excitation [2–4]. The excited ions typically decay by emission of one or more neutrons which move in the longitudinal direction with approximately the same momentum as the beam. This process has a distinctive event signature.

In this Letter, we consider vector-meson production accompanied by mutual Coulomb dissociation, as shown in Fig. 1. More generally, we discuss the use of mutual dissociation as a "tag" of impact parameter. The vector-meson calculations follow the model for exclusive production in Ref. [5]. Vector-meson production accompanied by mutual excitation has a different impact parameter distribution than exclusive production, and this alters both the rapidity and transverse-momentum distributions.

The diagram in Fig. 1, corresponding to exchange of three photons, is dominant for vector-meson production in coincidence with Coulomb breakup. For factorization to hold, these photons must be emitted independently. This was demonstrated by Gupta [6].

Calculations in Ref. [7] have shown that the probability of a photon leaving the emitting nucleus in an excited state is small for the case of heavy-ion two-photon particle production. It is even less likely that the scattering represented by the dashed line in Fig. 1 will excite the emitting nucleus. One important difference between two-photon interactions and coherent vector-meson production is that the meson scatters from neutrons as well as protons. In a giant dipole resonance (GDR) the protons and neutrons oscillate against each other, so a force with equal coupling to protons and neutrons should not excite a GDR. The equicoupling to neutrons and protons also holds for the $C = +$ mesons (mostly the f_1 and a_2) which can interact with a photon to produce vector mesons.

These theoretical arguments are supported by data. The STAR Collaboration has observed ρ production with and without nuclear excitation, in gold-gold collisions at an energy of $\sqrt{s_{NN}} = 130$ GeV per nucleon. The ρ data with excitation was collected with a trigger based on mutual excitation, while the exclusive ρ sample was collected with a low-multiplicity charged particle trigger [8]. Both ρ spectra are similarly peaked for $p_T < 100$ MeV/c.

The Weizsäcker-Williams photon spectrum at a perpendicular distance b from the center of the emitting nucleus

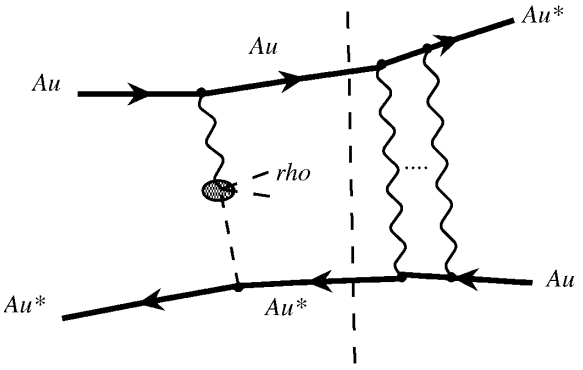

FIG. 1. The dominant Feynman diagrams for vector-meson production with nuclear excitation.

is [9–11]

$$\frac{d^3n(b,k)}{dkd^2b} = \frac{Z^2\alpha}{\pi^2 k}\left|\int_0^\infty dk_\perp\, k_\perp^2 \times \frac{F^2(k_\perp^2 + k^2/\gamma^2)k_\perp^2}{\pi^2(k_\perp^2 + k^2/\gamma^2)^2} J_1(bk_\perp)\right|^2, \quad (1)$$

where $\alpha \sim 1/137$ is the electromagnetic coupling constant, k is the photon energy, and $k_\perp$ is the photon transverse momentum with respect to the direction of nuclear motion. Here, J_1 is a Bessel function, and γ the Lorentz boost in the target frame. For a collider, γ is related to the lab-frame boost γ_{cm} by $\gamma = 2\gamma_{cm}^2 - 1$. For heavy nuclei, the nuclear charge form factor F can be analytically modeled by the convolution of a hard sphere with a Yukawa potential of range 0.7 fm [5].

The probability of having a mutual Coulomb excitation in a collision with impact parameter b is calculated along the same lines as in [3]. For low-energy photons ($k < \sim$30 MeV in the target frame), the dominant photonuclear reaction is excitation of the target to a GDR. This collective excitation usually decays by single neutron emission, with multiple neutron emission also possible [12]. Higher-energy photons can excite the nucleus to higher collective modes or excite individual nucleons (i.e., via $\gamma p \to \Delta$). More energetic interactions generally lead to multiple neutron emission, sometimes accompanied by π emission.

This Letter treats two cases: a general Coulomb excitation leading to the emission of any number of neutrons (Xn) and an excitation to a GDR followed by the emission of exactly one neutron ($1n$). The lowest-order probability for an excitation to any state which emits one or more neutrons (Xn) is

$$P^1_{C(Xn)}(b) = \int dk\, \frac{d^3n(b,k)}{dkd^2b}\, \sigma_{\gamma A\to A^*}(k)\,. \quad (2)$$

Here, the superscript 1 shows that this is the lowest-order probability. The photoexcitation cross section $\sigma_{\gamma A\to A^*}(k)$ is determined by measurements [13].

At small impact parameters, $P^1_C(b)$ can exceed 1 and so cannot be interpreted as a probability. Instead, it corresponds to the mean number of excitations. The excitation probability may be determined by a unitarization procedure. The probability of having exactly N excitations follows a Poisson distribution

$$P_N(b) = \frac{[P^1(b)]^N \exp[-P^1(b)]}{N!}\,. \quad (3)$$

The probability of having at least one Coulomb excitation is then $P_{C(Xn)}(b) = 1 - \exp[-P^1_{C(Xn)}(b)]$.

The probability of excitation followed by single neutron emission may be similarly determined. Here, the lowest-order probability is determined as in Eq. (2), except that the photon energy integration is truncated at the maximum GDR energy, and data on photoemission of single neutrons is used, avoiding uncertainties about the GDR branching ratios. For single neutron emission, there must be a single $1n$ excitation, unaccompanied by higher excitations. So, $P_{C(1n)}(b) = P^1_{C(1n)}(b)\exp[-P^1_C(b)]$.

In mutual dissociation, each individual breakup occurs independently [2]. The probability is thus the square of the individual breakup probabilities, i.e., $P_{C(XnXn)}(b) = [P_{C(Xn)}(b)]^2$ and $P_{C(1n1n)}(b) = [P_{C(1n)}(b)]^2$. Mutual dissociation is an experimental signature for low-b events [8]. When a nucleus breaks up, the neutron momentum is largely unchanged, and so the neutrons are detectable in zero degree calorimeters [3,14,15].

Vector mesons are produced in peripheral heavy-ion interactions through coherent interactions [5,8]. A photon from the field of one nucleus fluctuates to a quark-antiquark pair and scatters elastically from the other nucleus, emerging as a vector meson. The cross section is sensitive to the vector meson-nucleon interaction cross section. The photon energy k is related to the final state meson rapidity, $y = 1/2\ln(2k/M_V)$, where M_V is the vector-meson mass. Since the photon energy spectrum depends on b, the meson rapidity distribution $d\sigma/dy$ also varies with b. A vector meson can be produced at either ion and thus the two ions act as a two-source interferometer [16].

The probability for vector-meson production $P_V(b)$ is similar to that for nuclear excitation, except that $P_V(b)$ is small, so there is no need for a unitarization process:

$$P_V(b) = \int dk\, \frac{d^3n(b,k)}{dkd^2b}\, \sigma_{\gamma A\to VA}(k)\,. \quad (4)$$

$P_V(b)$ is the probability for producing a vector meson at one nucleus. The total probability is obtained by doubling P_V to take into account that either nucleus can emit a photon. This factor of 2 was not present for dissociation because Eq. (3) and our subsequent expressions for $P_{C(Xn)}(b)$ and $P_{C(1n)}(b)$ were for excitation of a specific nucleus. The natural width of the ρ^0 is included [5].

Assuming that the subreactions are independent, the cross section to produce a vector meson accompanied by mutual dissociation is

$$\sigma(AA \to A^*A^*V) = 2\int d^2b\, P_V(b) P_{XnXn}(b) \times \exp[-P_H(b)]\,. \quad (5)$$

$P_H(b)$ is the mean number of projectile nucleons that interact at least once:

$$P_H(b) = \int d^2\vec{r}\, T_A(\vec{r} - \vec{b})\{1 - \exp[-\sigma_{NN}T_B(\vec{r})]\}\,. \quad (6)$$

The nuclear thickness function, $T(\vec{r})$, is calculated from the nuclear density distribution and total nucleon-nucleon cross section $\sigma_{NN} = 52$ mb (88 mb) at a center of mass energy of 200 GeV (5.5 TeV) per nucleon pair [3,5]. The factor $\exp[-P_H(b)]$ in Eq. (5) ensures that the reaction is unaccompanied by hadronic interactions. For a solid-sphere nucleus model, the hadronic interaction probability is 1 for $b < 2R_A$ and is zero otherwise. Here, we calculate the interaction probability from a Glauber model.

TABLE I. Cross sections and median impact parameters b_m, for production of vector mesons.

Meson	Overall		$XnXn$		$1n1n$	
	σ (mb)	b_m (fm)	σ (mb)	b_m (fm)	σ (mb)	b_m (fm)
			Gold beams at RHIC ($\gamma_{cm} = 108$)			
ρ^0	590	46	39	18	3.5	19
ω	59	46	3.9	18	0.34	19
ϕ	39	38	3.1	18	0.27	19
J/ψ	0.29	23	0.044	17	0.0036	18
			Lead beams at LHC ($\gamma_{cm} = 2940$)			
ρ^0	5200	280	210	19	12	22
ω	490	290	19	19	1.1	22
ϕ	460	220	20	19	1.1	22
J/ψ	32	68	2.5	19	0.14	21

Table I gives the production cross sections and median impact parameters b_m for the different tags, as calculated from Eq. (5). The $XnXn$ and $1n1n$ cross sections are about $1/10$ and $1/100$ of the untagged cross sections, respectively.

Figure 2 compares the probability of ρ production as a function of impact parameter for $XnXn$ and $1n1n$ excitation and also without requiring nuclear excitation for (a) gold-gold collisions at a center of mass energy $\sqrt{s_{NN}} =$ 200 GeV per nucleon, as are found at the Relativistic Heavy Ion Collider (RHIC) at Brookhaven National Laboratory, and for (b) lead-lead collisions at $\sqrt{s_{NN}} = 5.5$ TeV per nucleon as are planned at the Large Hadron Collider (LHC) at CERN. These curves were obtained by evaluating the integrand of Eq. (5) at different b. The b distributions are very different for tagged and untagged ρ production; this is reflected in the vastly different b_m in Table I. The $1n1n$ and $XnXn$ spectra are closer, except that $XnXn$ is more strongly peaked for $b < 20$ fm, likely reflecting the increased phase space for high-energy excitations there. With nuclear breakup, b_m is almost independent of the final state vector meson.

Figure 3 shows the rapidity distribution $d\sigma/dy$ for ρ and J/ψ production at RHIC and the LHC. Spectra for $XnXn$ and $1n1n$ breakup are shown, along with the untagged $d\sigma/dy$. The $d\sigma/dy$ are symmetric around $y = 0$ because either nucleus can emit the photon. Since the photon spectrum falls as $1/k$ and $y = 1/2 \ln(2k/M_V)$, the

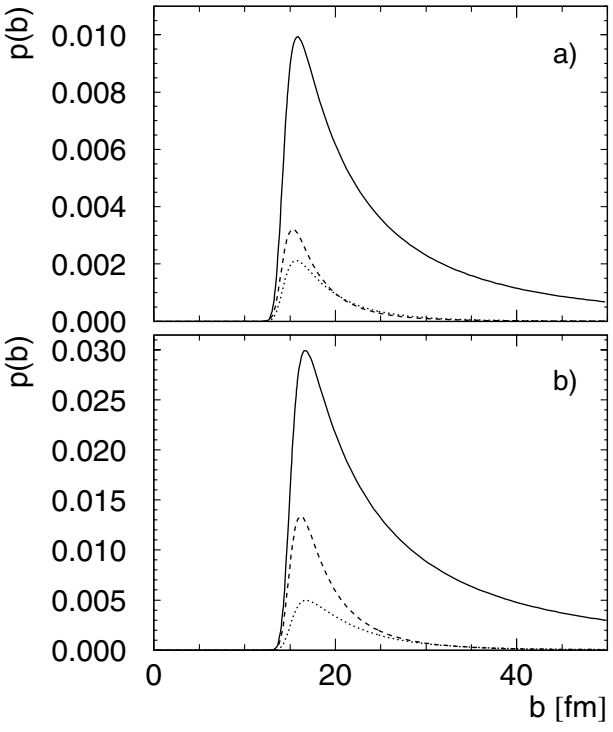

FIG. 2. The probability of ρ^0 production with (a) gold beams at RHIC and (b) lead beams at the LHC as a function of b, with $XnXn$ (dashed curve) and $1n1n$ (dotted curve) and without nuclear excitation (solid curve). The $1n1n$ curve is multiplied by 10 to fit on the plot.

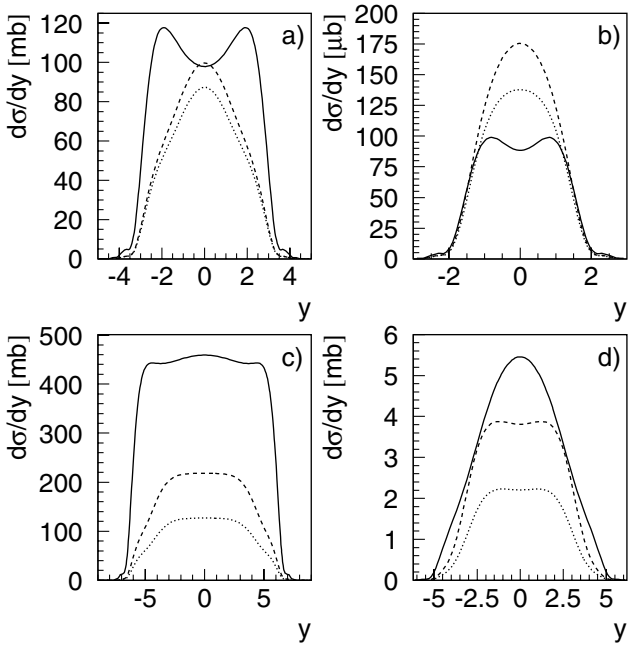

FIG. 3. Rapidity spectrum $d\sigma/dy$ for (a) ρ production at RHIC, (b) J/ψ production at RHIC, (c) ρ production at LHC, and (d) J/ψ production at the LHC. The solid line is the total production, the dashed line is for $XnXn$, multiplied by 10, and the dotted line is $1n1n$, multiplied by 100.

vector meson is usually in the hemisphere that the photon came from, with large $|y|$ corresponding to low photon energies. The tagged spectra have a smaller $|y|$ than the untagged distribution, with a small difference between the $XnXn$ and $1n1n$ calculations. Breakup preferentially selects collisions with smaller impact parameters, with higher median photon energies, and so the vector mesons are produced closer to midrapidity.

The form factor for a nucleus in an excited (i.e., GDR) state may be different from ground state nuclei. This could conceivably affect the vector-meson production, particularly the meson p_t spectra. However, this should at most be a small effect and we neglect it here.

The meson p_T spectrum also depends on b. For production at a single source (target nucleus), the meson p_T is the sum of the photon and scattering p_T, which is largely independent of b. The photon p_T comes from the equivalent photon approximation, (2), while the p_T from the coherent scattering depends directly on the form factor, Eq. (2) of Ref. [16]. The overall meson p_T spectrum is affected by interference from the two production sources (ions). The two amplitudes add with a b-dependent phase factor $\exp(i\vec{p}_T \cdot \vec{b})$. At midrapidity the two amplitudes have the same magnitude but the opposite sign, because of the negative parity of the vector meson, and

$$\sigma(p_T, b) = \sigma_1(p_T, b)[1 - \cos(\vec{p}_T \cdot \vec{b})], \qquad (7)$$

where $\sigma_1(p_T, b)$ is the cross section for emission from a single source. Of course, $\vec{b}$ is unknown, so Eq. (7) must be integrated over $\vec{b}$. This integration washes out the interference term in Eq. (7) except for $p_T < \hbar/\langle b \rangle$, where the cross section is reduced. As $\langle b \rangle$ decreases, the interference extends to higher and higher p_T. In this way, tagging affects the p_T spectrum.

Figure 4 compares the p_T distributions, d^2N/dp_T^2 for ρ and J/ψ production at RHIC and the LHC. The solid line shows the untagged spectra, while the dashed and dotted lines are for $XnXn$ and $1n1n$, respectively. The differences are moderate at RHIC and large at the LHC, where the exclusive vector mesons can have much larger b_m than the tagged sample. The different distributions can be used to study interference under different conditions.

Although we have focused on b-tagging vector-meson production, this technique should also be useful for studying two-photon interactions at heavy ion colliders. Here, e^+e^- production is of special interest. At b smaller than the electron Compton wavelength, $\lambda_C = 386$ fm, the fields are very strong, and multiple pairs production is enhanced over single pair production [1]. Mutual excitation could be used to select events with $b < \lambda_C$ and to look for enhanced multiple pair production.

In conclusion, we have calculated the cross sections and rapidity and transverse momentum distributions for vector mesons accompanied by nuclear breakup. Nuclear breakup is an effective tag for events with smaller average b. These events will have different rapidity and p_t distributions from the untagged events and can be used to explore the effects of different photon spectra and b distributions.

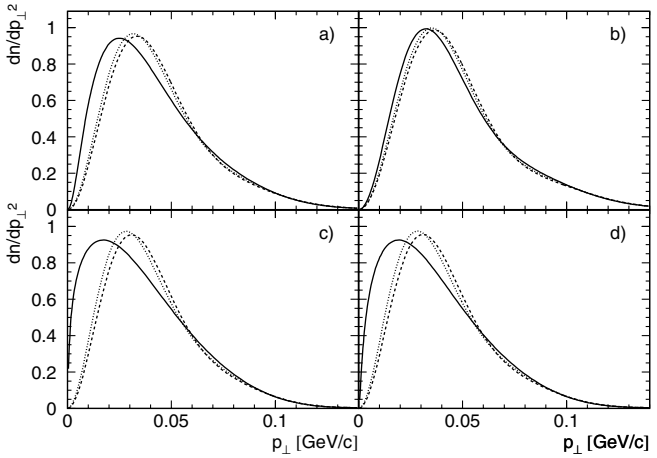

FIG. 4. The transverse momentum spectrum $d^2\sigma/dp_t^2$ at midrapidity, $y = 0$, for (a) ρ production at RHIC, (b) J/ψ production at RHIC, (c) ρ production at LHC, and (d) J/ψ production at the LHC. The solid line is the total production, the dashed line is for $XnXn$, and the dotted line is $1n1n$. All of the curves assume that there is interference and are normalized so that without interference $dn/dp_T^2 = 1$ at $p_T = 0$.

This work was supported by the U.S. Department of Energy under Contracts No. DE-AC-03076SF00098 and No. DE-AC02-98CH10886 and by the Swedish Research Council (VR).

[1] G. Baur, K. Hencken, and D. Trautmann, J. Phys. G **24**, 1657 (1998); C. A. Bertulani and G. Baur, Phys. Rep. **163**, 299 (1988).
[2] K. Hencken, D. Trautmann, and G. Baur, Phys. Rev. C **53**, 2532 (1996).
[3] A. J. Baltz, C. Chasman, and S. N. White, Nucl. Instrum. Methods Phys. Res., Sect. A **417**, 1 (1998).
[4] I. A. Pshenichnov *et al.,* Phys. Rev. C **64**, 024903 (2001).
[5] S. R. Klein and J. Nystrand, Phys. Rev. C **60**, 014903 (1999).
[6] S. N. Gupta, Phys. Rev. **99**, 1015 (1955).
[7] K. Hencken, D. Trautmann, and G. Baur, Z. Phys. C **68**, 473 (1995).
[8] S. Klein, nucl-ex/0104016.
[9] R. N. Cahn and J. D. Jackson, Phys. Rev. D **42**, 3690 (1990).
[10] G. Baur and L. G. Ferreira Filho, Nucl. Phys. **A518**, 786 (1990).
[11] M. Vidovic, M. Greiner, C. Best, and G. Soff, Phys. Rev. C **47**, 2308 (1993).
[12] N. Baron and G. Baur, Phys. Rev. C **48**, 1999 (1993); M. Vidovic, M. Greiner, and G. Soff, Phys. Rev. C **48**, 2011 (1993).
[13] A. J. Baltz, M. J. Rhoades-Brown, and J. Weneser, Phys. Rev. E **54**, 4233 (1996).
[14] M. Chiu *et al.,* nucl-ex/0109018.
[15] C. Adler *et al.,* Nucl. Instrum. Methods Phys. Res., Sect. A **461**, 337 (2001).
[16] S. R. Klein and J. Nystrand, Phys. Rev. Lett. **84**, 2330 (2000).